Biochimica et Biophysica Acta 1851 (2015) 220–230

Contents lists available at ScienceDirect

Biochimica et Biophysica Acta

journal homepage: www.elsevier.com/locate/bbalip

Role of long-chain acyl-CoA synthetase 4 in formation of polyunsaturated lipid species in hepatic stellate cells

Maidina Tuohetahuntila [a], Bart Spee [b], Hedwig S. Kruitwagen [b], Richard Wubbolts [a], Jos F. Brouwers [a], Chris H. van de Lest [a], Martijn R. Molenaar [a], Martin Houweling [a], J. Bernd Helms [a], Arie B. Vaandrager [a,*]

[a] Department of Biochemistry and Cell Biology, Faculty of Veterinary Medicine & Institute of Biomembranes, Utrecht University, Yalelaan 2, 3584 CM Utrecht, The Netherlands
[b] Department of Clinical Sciences of Companion Animals, Faculty of Veterinary Medicine, Utrecht University, Yalelaan 104, 3584 CM Utrecht, The Netherlands

ARTICLE INFO

Article history:
Received 15 September 2014
Received in revised form 17 November 2014
Accepted 1 December 2014
Available online 9 December 2014

Keywords:
Prostaglandin
Eicosanoid
Phosphatidylcholine
Lipidomics
Heavy isotope labeling
Arachidonic acid

ABSTRACT

Hepatic stellate cell (HSC) activation is a critical step in the development of chronic liver disease. We previously observed that the levels of triacylglycerol (TAG) species containing long polyunsaturated fatty acids (PUFAs) are increased in in vitro activated HSCs. Here we investigated the cause and consequences of the rise in PUFA-TAGs by profiling enzymes involved in PUFA incorporation. We report that acyl CoA synthetase (ACSL) type 4, which has a preference for PUFAs, is the only upregulated ACSL family member in activated HSCs. Inhibition of the activity of ACSL4 by siRNA-mediated knockdown or addition of rosiglitazone specifically inhibited the incorporation of deuterated arachidonic acid (AA-d8) into TAG in HSCs. In agreement with this, ACSL4 was found to be partially localized around lipid droplets (LDs) in HSCs. Inhibition of ACSL4 also prevented the large increase in PUFA-TAGs in HSCs upon activation and to a lesser extent the increase of arachidonate-containing phosphatidylcholine species. Inhibition of ACSL4 by rosiglitazone was associated with an inhibition of HSC activation and prostaglandin secretion. Our combined data show that upregulation of ACSL4 is responsible for the increase in PUFA-TAG species during activation of HSCs, which may serve to protect cells against a shortage of PUFAs required for eicosanoid secretion.

1. Introduction

Hepatic stellate cells (HSCs)[1] are non-parenchymal cells which are located in the spaces of Disse, between the sinusoidal endothelial cells and the hepatocytes [1,2]. In a healthy liver, HSCs are involved in vitamin A (retinol) homeostasis as they are filled with large LDs containing retinylesters, together with triacylglycerols (TAGs) and cholesteryl esters. HSCs also play a role in the turnover of hepatic extracellular matrix (ECM) components such as collagen, glycoprotein and proteoglycan [3]. HSC proliferation and collagen synthesis are regulated by the 3D structure of the ECM [4]. Upon liver injury, quiescent HSCs can transdifferentiate into an activated myofibroblastic phenotype. Activated Kupffer cells may initiate this transition by secreting cytokines, such as transforming growth factor beta (TGF-β), which stimulate the synthesis of matrix proteins and the release of retinoids by HSCs [5]. Production of TGF-β by activated HSCs further stimulates the excess synthesis of ECM and results in liver fibrosis [6].

We previously reported that LD degradation in activated hepatic stellate cell is a highly dynamic and regulated process [7]. Upon activation of the hepatic stellate cells, the LDs reduce in size, but increase in number during the first 7 days in culture. The LDs migrate to cellular extensions in this first phase, before they disappear in a later phase. Raman and lipidomic studies showed that in the initial phase of HSC activation, the retinyl esters are disappearing more rapidly than the triacylglycerols. Interestingly, a large and specific increase in polyunsaturated fatty acid (PUFA)-containing triacylglycerol species was observed during the first 7 days in culture, together with the decrease in retinyl esters [7]. The increase in PUFA-TAGs was caused by a large increase in the uptake of PUFAs from the medium as assessed from deuterium-labeled arachidonic acid uptake studies [7]. So far, the molecular mechanisms and identity of the enzymes involved in the lipid remodeling and breakdown of the LDs during HSC activation are unknown. In this study, we aim to identify lipid enzymes responsible for the accumulation of PUFA-TAG species in activated HSCs and their possible role in the activation or function of HSCs. Our initial targets were isoforms of the family of acyl-CoA synthetases (ACSLs). Members of this family are key enzymes in the synthesis of complex lipids like

Abbreviations: HSC, hepatic stellate cell; LD, lipid droplet; TAG, triacylglycerol; ACSL, long-chain acyl-CoA synthetase; PC, phosphatidylcholine; AA, Arachidonic acid; AA-d8, deuterated arachidonic acid; PL, phospholipid

* Corresponding author at: Dept. Biochemistry and Cell Biology, Utrecht University, Faculty of Veterinary Medicine, Yalelaan 2, 3584 CM Utrecht, The Netherlands. Tel.: +31 30 2535378; fax: +31 30 2535492.
E-mail addresses: T.Maidina@uu.nl (M. Tuohetahuntila), B.Spee@uu.nl (B. Spee), H.S.Kruitwagen@uu.nl (H.S. Kruitwagen), r.wubbolts@uu.nl (R. Wubbolts), j.brouwers@uu.nl (J.F. Brouwers), C.H.A.vandeLest@uu.nl (C.H. van de Lest), m.r.molenaar@uu.nl (M.R. Molenaar), M.Houweling@uu.nl (M. Houweling), J.B.Helms@uu.nl (J.B. Helms), A.B.Vaandrager@uu.nl (A.B. Vaandrager).

http://dx.doi.org/10.1016/j.bbalip.2014.12.003
1388-1981/

phospholipids (PLs), cholesterol esters and TAGs by converting free long-chain fatty acids into acyl-CoAs [8]. Furthermore, uptake of long chain fatty acids is tightly linked to CoA-esterification by acyl-CoA synthetases. Five isoforms of ACSL have been identified in mammals. The ACSL family members differ in their specificity for fatty acid species and in their tissue distributions. Among the ACSLs, ACSL4 is a peripheral membrane protein that was found to be selective for arachidonic acid (AA) and other longer chain polyunsaturated fatty acids and is highly expressed in adrenal gland, brain, ovary and testis [9].

The identification of the enzyme responsible for the increase in PUFA-TAGs will allow us to investigate the role of these lipids in the functioning of HSCs. Elevation of TAG-PUFA species may be physiologically relevant as storage pools for AA, waiting to be incorporated in PLs. AA is also a precursor for eicosanoids, which are signaling lipids that play a role in a broad range of processes, such as modulation of inflammation and the immune system [10,11]. Eicosanoid synthesis typically starts with the release of AA from the sn-2 position of PLs by specific Ca^{2+}-dependent phospholipases in response to hormones/cytokines [12]. Subsequently AA is converted to various eicosanoids, like prostaglandins, thromboxanes or leukotrienes, depending on the relative activity of their respective synthases.

Here, we report that ACSL4 upregulation is critically involved in the increase in TAG-PUFA formation in activated HSCs, which may serve as a storage pool for eicosanoid production.

2. Materials and methods

2.1. Reagents

AA-d8 was purchased from Cayman Chemical (Ann Arbor, MI, USA). 15-deoxy-Δ12,14 prostaglandin J2 (15-dPGJ2) was from Tocris Bioscience (United Kingdom). Dulbecco's modified Eagle medium (DMEM), fetal bovine serum (FBS), and penicillin/streptomycin were obtained from Gibco (Paisley, UK). Bovine Serum Albumin (BSA) fraction V was obtained from PAA (Pasching, Austria). Rosiglitazone was obtained from Enzo Life Sciences (Belgium). Collagenase (Clostridium histolyticum Type I) was obtained from Sigma-Aldrich (St. Louis, MO, USA). Anti-rabbit IgG ACSL4 antibody was from Santa Cruz Biotechnology (Santa Cruz, CA, USA). The antibody against alpha-smooth muscle actin (α-SMA) was from Thermo Scientific (Waltham, MA, USA), and mouse monoclonal anti-tubulin antibody from Sigma-Aldrich (St. Louis, MO, USA). Lipid droplet staining dye LD540 was kindly donated by Dr. C. Thiele, Bonn, Germany. Hoechst 33342 was obtained from Molecular Probes (Paisley, UK), paraformaldehyde (PF) (8%) was obtained from Electron Microscopy Sciences (Hatfield, PA, USA). FluorSave was obtained from Calbiochem (Billerica, MA, USA), all HPLC-MS solvents were from Biosolve (Valkenswaard, the Netherlands) with exception of chloroform (Carl Roth, Karlsruhe, Germany) and were of HPLC grade. Silica-G (0.063–0.200 mm) was purchased from Merck (Darmstadt, Germany).

2.2. Animals

Procedures of rat care and handling were in accordance with governmental and international guidelines on animal experimentation, and were approved by the Animal Experimentation Committee (Dierexperimentencommissie; DEC) of Utrecht University (DEC-numbers: 2010.III.09.110 and 2012. III.10.100).

2.3. Cell line

Human hepatic stellate cell line (LX-2) was kindly donated by Dr. Friedman (New York, NY, USA). LX-2 cells were cultured in DMEM medium supplemented with 10% FBS, 100 units/ml penicillin, and 100 μg/ml streptomycin and cells were maintained in a humidified 5% CO_2 incubator at 37 °C.

2.4. Rat HSC isolation and in vitro primary cell culture

Adult male Wistar rats (300–400 g) were used in all experiments. Stellate cells were isolated from rat liver by collagenase digestion followed by differential centrifugation [13]. After isolation, HSCs were plated in 24, 12 or 6 well plates at a density of 2×10^4, 5×10^4 or 1×10^5 cells/well, respectively. Cells were maintained in DMEM supplemented with 10% FBS, 100 units/ml penicillin, 100 μg/ml streptomycin and 4 μl/ml Fungizone and cells were maintained in a humidified 5% CO_2 incubator at 37 °C. Medium was changed every 3 days. Purity of the HSC preparation as determined by desmin staining was 80–90%.

2.5. Gene silencing of Acsl4

Gene-silencing experiments were performed using small interfering RNA (siRNA) for *Acsl4* or non-targeting siRNA as a control (ON-TARGETplus SMARTpool of 4 siRNAs, Thermo-Scientific, Rochester, NY, USA) according to the manufacturer's instructions. Briefly, two days after plating, the cells were treated with 40 nM siRNA using 5 μl/ml RNAiMAX (Invitrogen, Breda, the Netherlands) in antibiotic free complete media (with FBS). After 6 h of transfection, media was changed to standard culturing conditions up to day 7.

2.6. RNA isolation, cDNA synthesis and QPCR

Total RNA was isolated from rat HSCs grown in a 24-well plate using RNeasy Mini Kit (Qiagen, Venlo, the Netherlands) including the optional on-column DNase digestion (Qiagen RNase-free DNase kit). RNA was dissolved in 30 μl of RNase free water and was quantified spectrophotometerically using a Nanodrop ND-1000 (Isogen Life Science, IJsselstein, the Netherlands). An iScript cDNA Synthesis Kit (Bio-Rad, Veenendaal, the Netherlands) was used to synthesize cDNA. Primer design and qPCR conditions were as described previously [14]. Briefly, qPCR reactions were performed in duplicate using Bio-Rad detection system. Amplifications were carried out in a volume of 25 μl containing 12.5 μl of 2xSYBR green supermix (BioRad), 1 μl of forward and reverse primer and 1 μl cDNA. Cycling conditions were as follows: initial denaturation at 95 °C for 3-minute, followed by 45 cycles of denaturation (95 °C for 10 s), annealing temperature (see Supplementary Table S1) for 30 s, and elongation (72 °C for 30 s). A melting curve analysis was performed for every reaction. To determine relative expression of a gene, a 4-fold dilution series from a pool of all samples were used. IQ5 Real-Time PCR detection system software (BioRad) was used for data analysis. Expression levels were normalized by using the average relative amount of the housekeeping genes. Housekeeping genes used for normalization are, based on their stable expression in stellate cells, namely, *tyrosine 3-monooxygenase/tryptophan 5-monooxygenase activation protein, zeta (Ywhaz)*, *hypoxanthine phosphoribosyl transferase (Hprt)*, and *hydroxylmethylbilane synthase (Hmbs)*. Primers for housekeeping genes and genes of interest are listed in Supplementary Table S1.

2.7. Western blot analysis

Cell homogenates were collected and equal amounts of proteins were heated to 95 °C for 5 min in loading buffer and then separated on 10% SDS-polyacrylamide gel and blotted onto polyvinylidene difluoride membranes (GE Healthcare Europe GmbH, Belgium). The membranes were incubated with 5% BSA in Tris-buffered saline (TBS) for 30 min at room temperature. The incubation of the primary antibody was performed at 4 °C overnight for all antibodies (see Supplementary Table S2) in TBS with 0.1% Tween-20 (Boom B.V., Meppel, the Netherlands) and 1% BSA. After washing, membranes were incubated with horseradish peroxidase-conjugated secondary antibody (Nordic Immunology, the Netherlands) at room temperature for 1 h. Blots

were detected by ECL kit (Supersignal West Pico; Pierce, Rockford, IL). Blots were then stripped in stripping buffer containing 100 mM 2-mercaptoethanol, 2% (w/v) SDS, 62.5 mM Tris–HCl (pH 6.7) and then probed with anti-tubulin antibody for protein content normalization. Imaging was performed on a ChemiDoc XRS System (BioRad). Western blot was performed in at least three different experiments, and representative blots are shown.

2.8. Immunofluorescence

Freshly isolated HSCs were grown on glass coverslips in 24 well plate untill day 1 or day 7 at 37 °C. In parallel, HSCs transfected at day 2 in culture with siRNAs targeted against *Acsl4* were grown until day 7 at 37 °C. Staining of cells was performed as follows: cells were fixed in 4% (v/v) PF at room temperature for 30 min and stored in 1% (v/v) PF at 4 °C for a maximum of 1 week. HSCs were washed twice in PBS, permeabilized (0.1% (w/v) saponin (PBS-S; Riedel-de Haën, Seelze, Germany)) and blocked with 2% BSA for 1 h at room temperature. After blocking, slides were incubated 1 h with the primary antibody against ACSL4 (4 μg/ml), washed again, and incubated for 1 h with anti-rabbit antibody (15 μg/ml) supplemented with Hoechst (4 μg/ml) for nuclear counterstaining and lipid droplet dye LD540 (0.05 μg/ml). Thereafter, coverslips were mounted with FluorSave on microscopic slides and Image acquisition was performed at the Center of Cellular Imaging, Faculty of Veterinary Medicine, Utrecht University, on a Leica TCS SPE-II confocal microscope. Images were adjusted in ImageJ (freeware available at www.download-imagej.com).

2.9. Analysis of neutral and phospholipids by HPLC-MS

Lipids were extracted from a total cell homogenate of HSCs grown in a 12-well plate by the method of Bligh and Dyer [15]. Extracted lipids were separated in a neutral and phospholipid fraction by fractionation on a freshly prepared silica-G column (approximately 10 mg of 0.063–0.200 mm silica) [16]. Lipid extracts were dissolved in methanol/chloroform (1/9, v/v) and loaded on top of the silica column. Neutral lipids were eluted with two volumes acetone, dried under nitrogen gas and stored at −20 °C. Just before HPLC-MS analysis, the neutral lipid fraction was reconstituted in methanol/chloroform (1/1, v/v) and separated on a Kinetex/HALO C8-e column (2.6 μm, 150 × 3.00 mm; Phenomenex, the Netherlands). A gradient was generated from methanol/H_2O (5/5, v/v) and methanol/isopropanol (8/2, v/v) at a constant flow rate of 0.3 ml/min. Mass spectrometry of neutral lipids (TAGs and cholesterol) was performed using Atmospheric Pressure Chemical Ionization (APCI) interface (AB Sciex Instruments, Toronto, ON, Canada) on a Biosystems API-2000 Q-trap. The system was controled by Analyst version 1.4.2 software (MDS Sciex, Concord, ON, Canada) and operated in positive ion mode using settings described in [7]. Absolute quantitation of all the TAG species was hampered by their sheer numbers (>1000) and the differential fragmentation of the various TAG species during ionization into DAG and MAG ions. The fragmentation depended on the saturation of the acyl chains, as almost no intact TAG ions were observed from TAGs with less than 2 double bonds, whereas some more unsaturated TAG species fragmented less than 40%. On average 40–50% of PUFA-containing TAGs were observed as intact ions. The fragmentation of specific TAG species was very reproducible between different samples, therefore we generally performed a relative quantitation of a number of abundant and representative TAG species. Typical TAG species quantitated were: non PUFA, 52:3 (m/z 859) and 54:3 (m/z 885); 1xPUFA, 56:5 (m/z 909) and 58:6 (m/z 935); 2xPUFA, 60:9 (m/z 957) and 62:11 (m/z 981). For the experiments with AA-d8 typical TAG species were: 1xPUFA-d8, 54:4 (m/z 881, 889), 56:5 (m/z 909, 917), 56:6 (m/z 907, 915), and 56:7 (m/z 905, 913); 2xPUFA-d8, 56:8 (m/z 903, 911, 919), 58:8 (m/z 931, 939, 947), 60:9 (m/z 957, 965, 973), and 3xPUFA, 60:12 (m/z 951, 959, 967, 975), and 62:12 (m/z 979, 987, 995, 1003). The quantitated TAG species were normalized to the amount of cholesterol in the same sample. Cholesterol was found to be a good marker for both recovery and cellular material, as the cholesterol/protein ratio was found to be constant during HSC culture. The phospholipid fraction was also dissolved in methanol/chloroform (1/1, v/v) and separated on a Kinetex/HALO C18-e column (2.6 μm, 150 × 3.00 mm; Phenomenex, the Netherlands). A gradient was generated from acetonitril/methanol/H_2O (6/9/5, v/v) and acetone/methanol (4/6, v/v) at a constant flow rate of 0.6 ml/min. Mass spectrometry of phosphatidylcholine (PC) was performed using electrospray ionization (ESI) on a Biosystems API-2000 Q-trap. The system was controled by Analyst version 1.4.2 software (MDS Sciex, Concord, ON, Canada) and operated in positive mode, precursor scan of 184 m/z, using settings described in [7].

2.10. Analysis of fatty acid constitution of neutral lipids and phospholipids

Total lipids from 400 μl of HSC homogenate were extracted using the method of Bligh and Dyer [15]. Internal standard (200 pmol of tripentadecanoylglycerol) was added to each sample prior to extraction to calculate absolute concentrations and the recovery. Subsequently, lipids were separated into a neutral and a phospholipid fraction according to [16] described as above on a silica-G column. Fractions were hydrolyzed at 75 °C for 1 h with 1 ml of MeOH:3 M NaOH (9:1, v/v) The released free fatty acids were obtained with extraction with hexane after subsequent acidification of the methanol phase according to [17], and evaporated under nitrogen and stored at −20 °C until analyzed. Mass spectrometry of free fatty acids was performed according to [18]. The system was controled by Analyst version 1.4.2 software (MDS Sciex, Concord, ON, Canada) and operated in negative mode in the m/z range from 225–400 amu. Calibration curves were generated using authentic standards to correct for differences in response factors. Data were expressed relative to the protein content of the homogenates as determined by the BCA method Pierce® BCA protein assay kit (Thermo scientific, Rockford, IL, USA) with BSA as standard.

2.11. Analysis of prostaglandins using mass spectrometry

DMEM containing 0.5% FBS with or without 10 μM Ca^{2+} ionophore A23187 was added to the HSCs 1 h before harvesting to reduce the background levels of eicosanoids present in serum. Eicosanoids were extracted and analyzed as described elsewhere with slight modifications [19]. Briefly, samples were recovered in a total volume of 1 ml of 15% (v/v) methanol + 0.5% glacial acetic acid in the presence of 10 pmol dimethyl-PGF2α that served as an internal standard. Samples were separated on on C18 solid-phase extraction columns. The eicosanoids were eluted with 2 × 0.35 ml ethyl acetate and evaporated to dryness under nitrogen. Evaporated samples were reconstituted with 50 μl of 50% ethanol and subject to HPLC–MS analysis. Multiple reaction monitoring (MRM) was used as described in [19].

2.12. Statistical analysis

Values for all measurements are expressed as mean ± SD. Each experiment was performed in duplicate and repeated at least three times. Comparisons between two groups were made with paired Student's *t* test. Differences were considered statistically significant if the P value was less than 0.05.

3. Results

3.1. Specific incorporation of arachidonic acid into triacylglycerol

When hepatic stellate cells (HSCs) become activated in culture, their levels of polyunsaturated triacylglycerol species (PUFA-TAGs) increase 4–5 fold, whereas the amounts of PUFA-containing PL species are not altered under the same conditions [7]. To investigate whether this

difference in PUFA accumulation between TAGs and PLs is caused by differential incorporation of exogenously added PUFAs, both quiescent (day 1) and activated (day 7) HSCs were incubated with 25 μM AA-d8 for 24 h. As shown in Fig. 1A, AA-d8 incorporation into TAGs was more than five times higher in activated HSCs compared to quiescent cells, in line with the previously reported increase in TAG-PUFA levels. In contrast, the overall AA-d8 incorporation into PC was already relatively high at day 1 and increased only modestly (less than 50%; Fig. 1B) in activated HSCs. This modest increase in deuterium-labeled PUFA PC was partly compensated by a decrease in non-labeled PUFA-PC resulting in overall small changes in PUFA-PC content during the 24 h incubation. These results corroborate that the increase in incorporation of PUFAs in activated HSCs is relatively specific for TAGs.

An exact determination of the contribution of the PUFA-TAG species to the total amount of TAG by the APCI-MS method is hampered by the numerous species (>1000) and the observation that the various TAG species fragment to a different degree depending on the saturation of their acyl chains as discussed in Section 2.9. Nevertheless, quantitation of a large number of intact and fragmented TAG ions resulted in a conservative estimate that HSCs at day 1 have 15–20% TAGs with one PUFA, 3–5% with two PUFAs, and <1% with three PUFAs. At day 7 these percentages increased to 30–40%, 20–30% and 6–10%, respectively. To alternatively determine the amount of PUFAs in the neutral lipid fraction, we hydrolyzed the neutral lipids and analyzed the fatty acids released. As shown in Fig. 1C and Supplementary Table S3, the percentage of PUFAs (defined as more than 20 C atoms and 3 double bonds) in HSCs increased from 25% to almost 50% after activation. The addition of 25 μM AA-d8 caused an even larger incorporation of PUFAs, resulting in the majority of the fatty acids in neutral lipids being a PUFA (Fig. 1C, Supplementary Table S3). The total amount of PUFAs in neutral lipids at day 7 (60–70 nmol/mg protein) was almost similar to the total amount of PUFAs in the phospholipid fraction (75–80 nmol/mg protein;

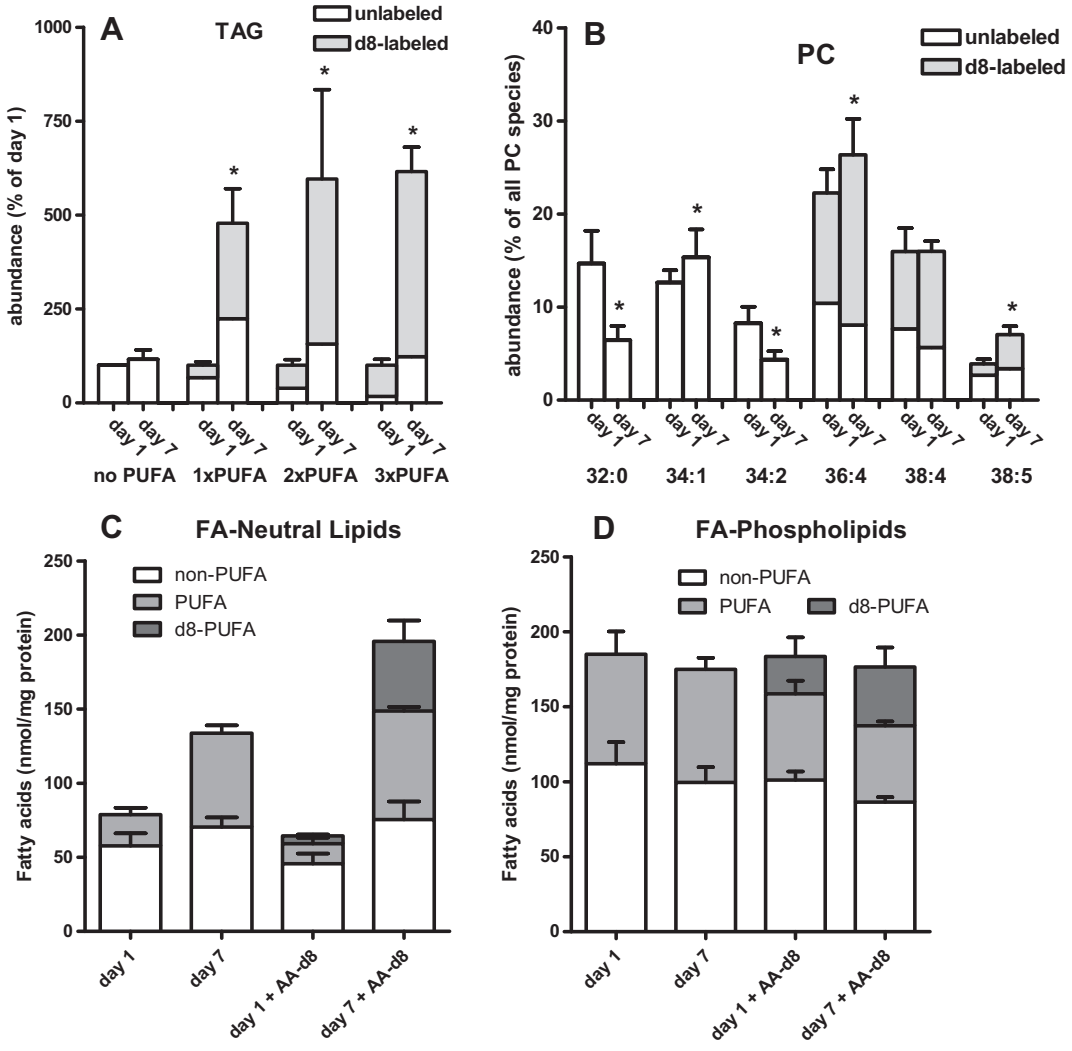

Fig. 1. Incorporation of arachidonic acid in activated HSCs. Freshly isolated HSCs were cultured for 1 or 7 days and additionally incubated for 24 h with 25 μM of AA-*d8* in medium with 10% FBS at 37 °C. Subsequently, neutral lipids and phospholipids were extracted and analyzed. A. Several representative TAG species with no, 1, 2, or 3 PUFA chains were quantified and unlabeled (white bars) and deuterium labeled variants (gray bars) of the same species were added. Values were normalized to the amount of cholesterol in the sample and expressed relative to the level of the respective TAG species present at day 1. B. The most abundant PC species were quantified, and unlabeled (white bars) and deuterium labeled variants (gray bars) of the same species were added. Values are expressed relative to the total amount of PC in a sample (which did not differ significantly between day 1 and day 7, when normalized to the amount of protein). Data are the means ± SD of 3 experiments performed in duplicate. *$P < 0.05$. C and D. Freshly isolated HSCs were cultured for 1 or 7 days and additionally incubated for 24 h without or with 25 μM of AA-*d8* in medium with 10% FBS at 37 °C. Subsequently, lipids were extracted, separated into a neutral (C) and a phospholipid (D) fraction, and hydrolyzed. The released fatty acids were analyzed with HPLC-MS. PUFAs are defined as fatty acids with 20 or more C atoms and 3 or more double bonds. Data are the means ± SD of 2 experiments performed in duplicate.

Fig. 1D, Supplementary Table S4). Fig. 1D also shows that the amount of PUFAs in the phospholipid fraction did not change upon activation of the HSCs, and that the addition of 25 μM AA-d8 rather caused a replacement of part of the PUFAs by labeled PUFAs, than a net increase in PL-PUFAs, similar as observed for PC (Fig. 1B).

3.2. ACSL4 is upregulated in activated HSCs

Uptake and incorporation of long-chain fatty acids is tightly linked to their CoA-esterification [8]. Therefore, to identify key enzymes involved in the enhanced formation of TAG-PUFA species in activated HSCs, we analyzed the expression of various acyl-CoA synthetases (ACSLs). As shown in Fig. 2A, the relative gene expression of all *Acsl* isoforms is downregulated two-fold or more in activated HSCs at day 7, except for the *Acsl4* isoform, which was upregulated approximately two-fold. This implies that *Acsl4* is enriched more than four-fold in relation to the other ACSL family members in activated HSCs when compared to quiescent HSCs. The increase in *Acsl4* mRNA was closely mirrored by the two-fold increase in ACSL4 protein as assessed by western blots (Fig. 2B). We next examined the subcellular localization of ACSL4 in

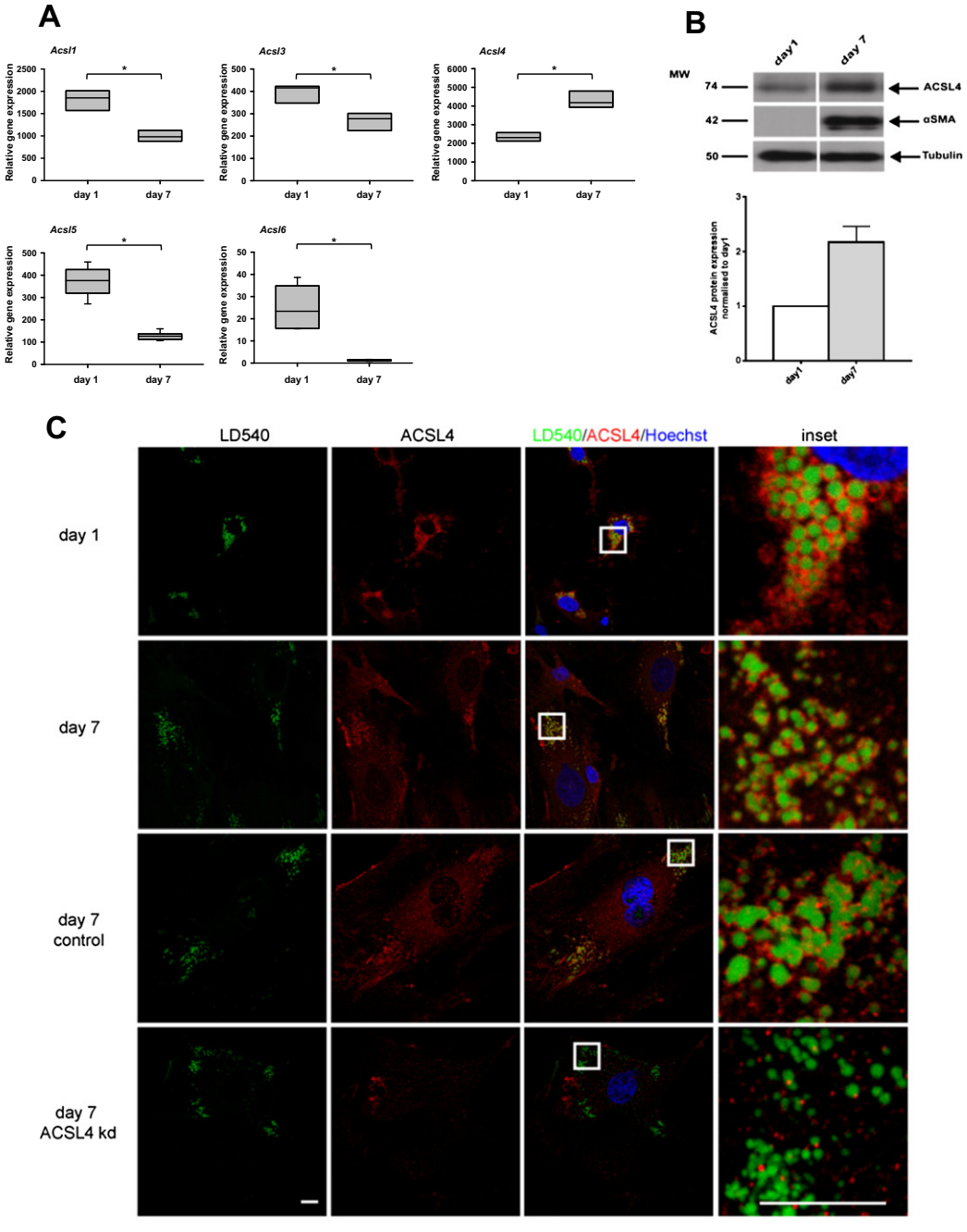

Fig. 2. ACSL4 upregulation in activated HSCs. A. Relative mRNA expression of ACSL isoforms in quiescent (day 1) and activated (day 7) rat HSCs by qPCR. The box plot depicts the median and lower and upper quartile ($n = 3$). Significant changes are marked by asterisks ($P < 0.05$). B. Protein expression was measured for ACSL4 in quiescent (day 1) and activated (day 7) rat HSCs by western blotting. αSMA was used as a positive control for HSC activation. Tubulin was used as a loading control. Shown is a representative blot and quantitation by densitometry of the ASCL4 band. Data are the means ± SD of 3 experiments C. Confocal images of ACSL4. Quiescent HSC (day 1) and activated HSC (day 7) lipid droplets were stained with LD540 dye (green), anti ACSL4 antibody (red) and nuclei were stained with Hoechst (blue). Colocalization of LDs with ACSL4 is shown in inset panel. Lower two panels: HSCs were transfected on day 2 with non-targeting siRNA or *Acsl4* siRNA and at day 7 stained as above. Images shown are representative for at least 3 independent experiments. Scalebars represent 10 μm.

activated and quiescent HSCs. In agreement with its involvement in TAG formation and remodeling, ACSL4 partially localizes around LDs in both quiescent and activated HSCs (Fig. 2C). The ACSL4 staining around the LDs was specific, since it was no longer observed after transfection with *Acsl4*-targeting siRNAs (Fig. 2C).

3.3. ACSL4 is involved in enhanced formation of PUFA-TAGs

Because ACSL4 is relatively specific for PUFAs [8] and it localizes to LDs, ACSL4 is a good candidate to mediate the increase in PUFA-TAG species in activated HSCs. To test this hypothesis, HSCs were transfected at day 2 in culture with siRNAs targeted against *Acsl4* and analyzed at day 7. Compared to non-targeting siRNA control, knockdown up to 70% with *Acsl4* siRNA was achieved on mRNA level and to 80–90% on the protein level (Fig. 3A). In order to ascertain whether ACSL*4* knockdown impaired incorporation of PUFAs in TAG, the siRNA-treated HSCs were incubated for 24 h with 25 μM AA-d8 and lipids were extracted and analyzed using HPLC-MS. As shown in Fig. 3B, ACSL *4* knockdown inhibited the incorporation of labeled AA into TAG. Especially the incorporation of two and three exogenous PUFA chains within the same TAG-species (2× and 3× PUFAs) was strongly inhibited. In contrast, ACSL*4* knockdown had little effects on the incorporation of exogenous AA into PC (see Fig. 3C), or into phosphatidylserine and phosphatidylinositol (data not shown).

To further examine the specific involvement of ACSL4 in PUFA metabolism in activated HSCs, cells were treated with rosiglitazone, a pharmacological drug well known for its ability to inhibit ACSL4 activity [20,21]. Initially, this inhibition was evaluated by determining the effect of rosiglitazone on the incorporation of exogenous AA-d8 into TAG species in the human stellate cell line LX-2. Rosiglitazone inhibited the incorporation of AA-d8 in the LX-2 cells with an IC_{50} of approximately 30 μM, and near maximal inhibition was reached at a concentration of 100 μM (results not shown). Subsequently a concentration of 100 μM rosiglitazone was used to determine its effect on AA-d8 incorporation in activated rat HSCs. As shown in Fig. 4A, in activated rat HSCs incorporation of two and three exogenous PUFA chains within the same TAG-species (2× and 3× PUFAs) was inhibited by more than 80% by rosiglitazone. The incorporation of only one PUFA into TAG was inhibited to a somewhat lesser degree, and incorporation of exogenous AA into PC was inhibited only marginally by pharmacological inhibition of ACSL4 (see Fig. 4).

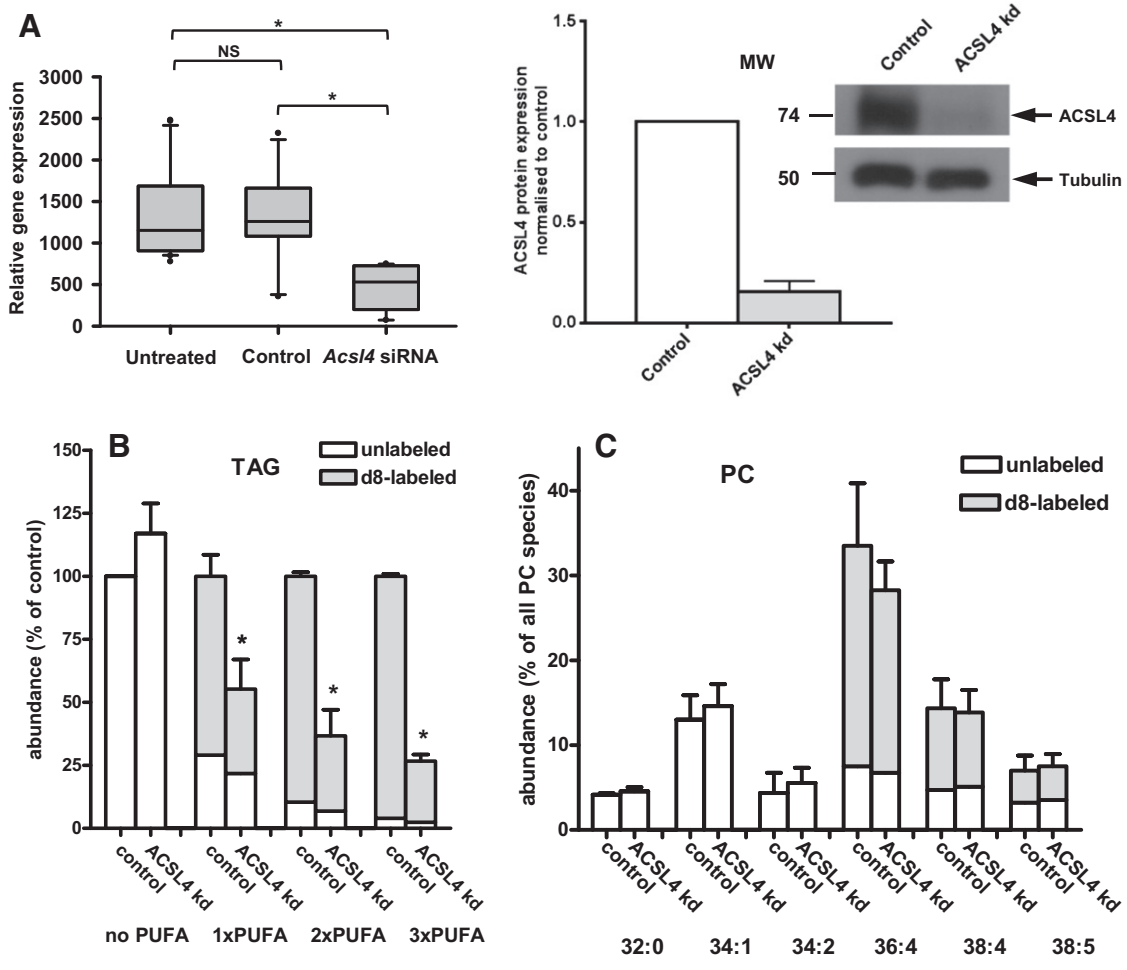

Fig. 3. *Acsl4* gene silencing reduces the incorporation of arachidonic acid into TAG. A. relative mRNA expression (left panel) and protein (right panel) of Acsl4 in HSCs 5 days after transfection with non-targeting (control) or *Acsl4* siRNA on day 2. Untreated sample represents untransfected HSCs cultured until day 7. NS, not significant. Significant changes are marked by asterisks ($P < 0.05$). Insert shows representative western blot. B, C. Isolated HSCs were transfected at day 2, and on day 6 incubated with 25 μM AA-d8 for 24 h. Cells were harvested on day 7. Subsequently, neutral lipids and phospholipids were extracted and HPLC-MS was performed as described. B. Several representative TAG species with no, 1, 2, or 3 PUFA chains were quantified and unlabeled (white bars) and deuterium labeled variants (gray bars) of the same species were added. Values were normalized to the amount of cholesterol in the sample and expressed relative to the level of the respective TAG species present in the non-targeting (control) cells. C. The most abundant PC species were quantified, and unlabeled (white bars) and deuterium labeled variants (gray bars) of the same species were added. Values are expressed relative to the total amount of PC in a sample (which did not differ significantly between non-targeting and *Acsl4* siRNA transfected cells). Data are the means ± SD of 3 experiments performed in duplicate. *$P < 0.05$ paired *t*-test.

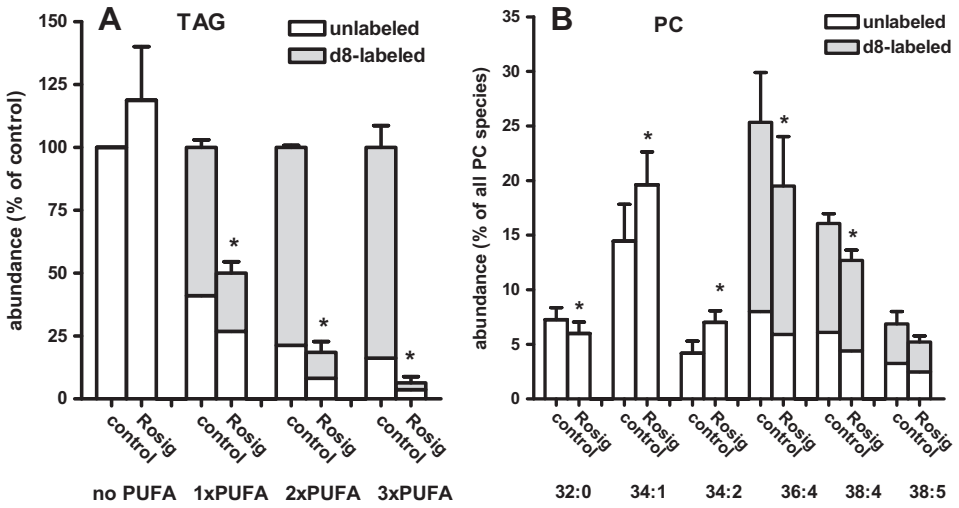

Fig. 4. Rosiglitazone inhibits arachidonic acid incorporation into TAG. Freshly isolated HSCs were cultured for 6 days. Subsequently the cells were incubated for 24 h with 25 μM AA-d8 in the absence (control) or presence of rosiglitazone (Rosig) (100 μM). Cells were harvested on day 7. Subsequently, neutral lipids and phospholipids were extracted and HPLC-MS was performed as described. A. Several representative TAG species with no, 1, 2, or 3 PUFA chains were quantified and unlabeled (white bars) and deuterium labeled variants (gray bars) of the same species were added. Values were normalized to the amount of cholesterol in the sample and expressed relative to the level of the respective TAG species present in the control cells. B. The most abundant PC species were quantified, and unlabeled (white bars) and deuterium labeled variants (gray bars) of the same species were added. Values are expressed relative to the total amount of PC in a sample. Data are the means ± SD of 3 experiments performed in duplicate. *$P < 0.05$ paired *t*-test. Rosiglitazone (Rosig) was added from a 25 mM stock in DMSO to final concentration of 100 μM (0.4% DMSO). In control experiments, the equivalent volume of DMSO was added.

3.4. Dose–response curve for the incorporation of exogenous AA into TAG and PC

We observed that in activated HSCs, the increased incorporation of PUFAs is relatively specific for TAG (Fig. 1) and that likewise, the inhibition of ACSL4 activity either by siRNA-mediated gene silencing or by rosiglitazone addition, affected the incorporation of AA into TAG to a larger extent than the incorporation of this PUFA into PC (Figs. 3 and 4). We questioned the reason for this differential incorporation since PUFA-CoA, the product of ACSL*4*, is the substrate for both PUFA-PC and PUFA-TAG synthesis. We investigated the possibility that the enzymes involved in the final step of PUFA-TAG and PUFA-PC synthesis have different affinities for PUFA-CoA. To probe the affinities of these enzymes we performed dose–response curves with exogenous AA-d8 at a relatively short incubation time during which the incorporation was linear with time. As shown in Fig. 5, AA-d8 was incorporated into PC and TAG species containing one molecule of AA-d8 with saturation kinetics fitting to a one binding site Michaelis–Menten model. The exogenous AA concentration at which half-maximal incorporation was observed was 4-fold higher for TAG as compared to PC (approx. 16 μM and 4 μM, respectively). In contrast, the incorporation of multiple AAs into one TAG molecule did not show saturation kinetics (within the concentration range studied), but increased with increasing exogenous AA concentrations. The different dose response curves show that different affinities of the final PC and TAG synthesizing enzymes for PUFAs are a possible explanation for the different responses of TAG and PC species profiles to changes in ACSL4 activity.

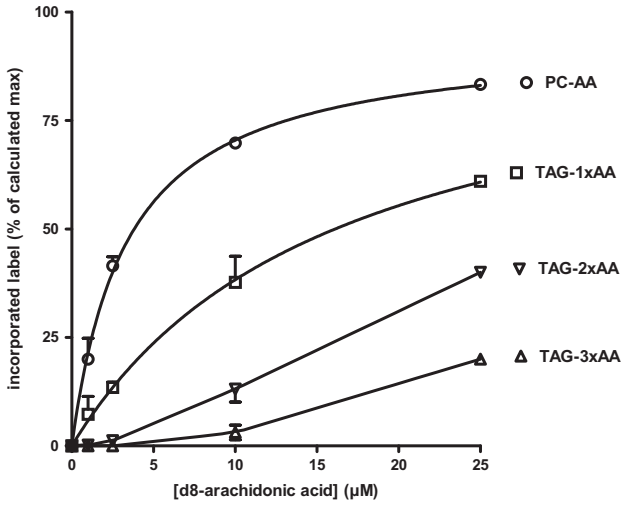

Fig. 5. Kinetics of arachidonic acid incorporated into PC and TAG. Freshly isolated HSCs were cultured for 7 days and additionally incubated with increasing concentrations of AA-d8 for another 3 h at 37 °C. Subsequently, lipids were extracted and HPLC-MS was performed as described. The d8-label in various representative TAG species with 1, 2 and 3 PUFAs (respectively TAG-1xAA, -2xAA, and -3xAA), and in the PC species 36:4, 38:4 and 38:5 (PC-AA) were quantified and summed. Data were fitted to one-site binding model (Michaelis–Menten plot) and the calculated Vmax was set as 100% in case of PC-AA and TAG-1xAA. TAG-2xAA and -3xAA data could not be fitted and were expressed relative to an arbitrary value. Data are the means ± SD of 3 experiments performed in duplicate.

3.5. Effect of ACSL4 inhibition on HSC lipid composition

To examine whether ACSL*4* plays a role in the overall lipid composition of HSCs activated in culture, we analyzed the endogenous TAG and PC species distribution after siRNA-mediated gene silencing of *Acsl4* or after inhibition of ACSL4 for 6 days with rosiglitazone. As shown in Fig. 6, the levels of the TAG-PUFAs were significantly lower in HSCs after the knock down of ACSL4 (see Fig. 6A). The levels of PC-species containing a PUFA were also reduced, but to a much lesser extent (Fig. 6B). The knock down of ACSL4 significantly decreased the ratio of PUFA-PC species to PC species without a PUFA from 1.40 ± 0.35 to 0.85 ± 0.30 ($n = 3$; $P < 0.01$ in paired *t*-test). We next questioned whether inhibition of ACSL*4* by rosiglitazone would lead to a similar difference in lipid profile in HSCs cultured for 7 days. As shown in Figs. 6C and D, addition of 100 μM rosiglitazone to isolated HSCs at day 1 changed the TAG-PUFA and PC-PUFA levels measured at day 7, causing more than 80% lower levels of PUFA-TAG species when compared to control. Rosiglitazone incubation also lowered the PUFA content of PC by approximately 50% (Fig. 6D). These experiments also show that prolonged inhibition of ACSL4 in the presence of relatively low levels of non-esterified AA (approx. 1–2 μM) present in medium

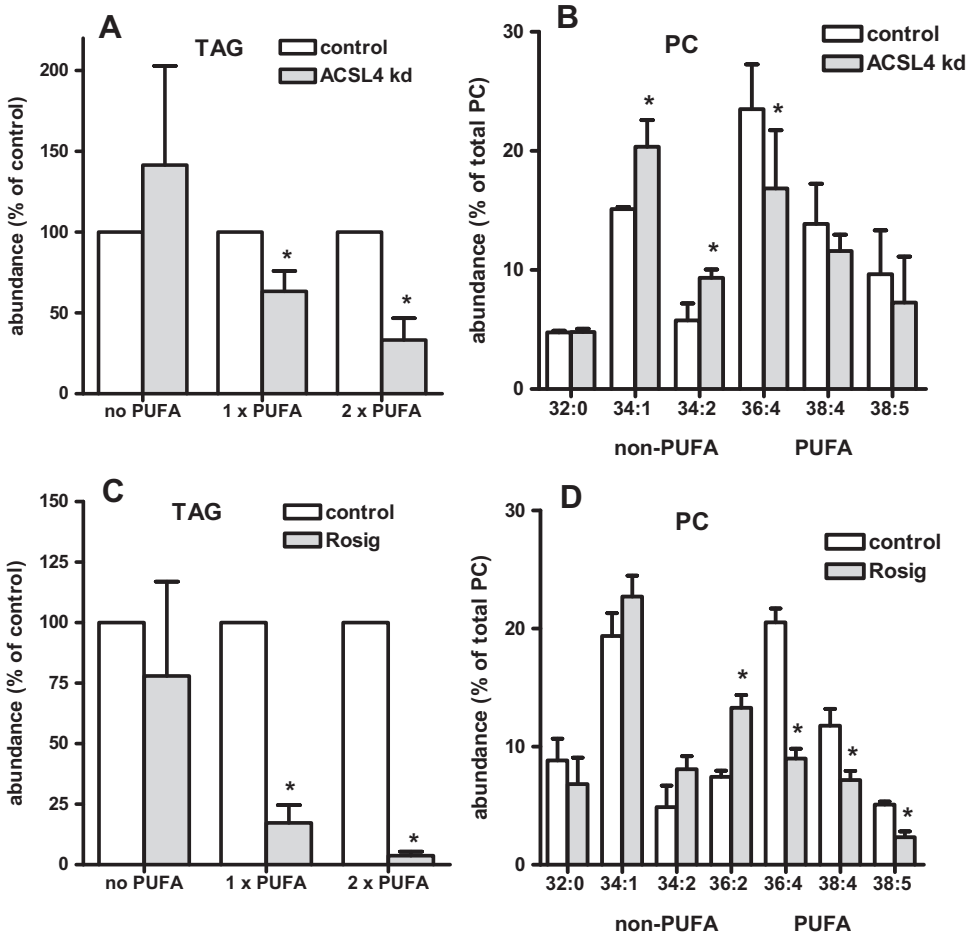

Fig. 6. The effect of ACSL*4* inhibition on endogenous lipids in activated HSCs. A,B. Freshly isolated HSCs were transfected with non-targeting (control) targetingor *Acsl4* siRNA at day 2 and cultured until day 7, or C,D isolated HSCs were incubated in the absence (control) or presence of rosiglitazone (Rosig) (100 μM) at day 1 and cultured in the continued presence of these substances until day 7. Subsequently, neutral lipids and phospholipids were extracted and HPLC-MS was performed as described. A,C. Several representative TAG species with no, 1, or 2 PUFA chains were quantified and normalized to the amount of cholesterol in the sample. Values and expressed relative to the level of the respective TAG species present in the non-targeting (control) cells (A), or control (C). B, D. The most abundant PC species were quantified and expressed relative to the total amount of PC in a sample. Data are the means ± SD of 3 experiments performed in duplicate. *P < 0.05 paired *t*-test. Rosiglitazone (Rosig) was added from a 25 mM stock in DMSO to final concentration of 100 μM. In control experiments, the equivalent volume of DMSO was added.

with 10% FBS also affects the levels of PC species containing AA, besides that of PUFA-TAGs. Thus, depending on the experimental conditions (high or low concentrations AA-d8), rosiglitazone had respectively little (Figs. 3B and 4B) or more substantial (Fig. 6D) effect on the incorporation of AA into PC.

3.6. Effect of ACSL4 inhibition on HSC activation

To investigate the role of the increased ACSL4 expression and the increase in PUFA-TAGs on HSC function, we determined the cellular morphology and levels of alpha-smooth muscle actin (αSMA) after knockdown of ACSL4 or pharmacological inhibition. αSMA is considered a marker for HSC activation [22] and was clearly upregulated in the HSCs after 7 days under our culture conditions (Fig. 2B). Treatment of HSCs with siRNA targeted against *Acsl4* on day 2 after plating did not cause a significantly different expression of αSMA mRNA (88 ± 18% compared to non-targeting siRNA (control) transfected; n = 4; non-significant), and no difference in cellular morphology was noted (Figs. 2C and D). However, the transfection with non-targeting siRNA already increased αSMA levels more than two-fold when compared to non-transfected cells, suggesting that the transfection procedure stimulated the activation process, and potentially masked an inhibitory role of ACSL4 knock down. Therefore the effect of rosiglitazone was also assessed on αSMA expression. As shown in Fig. 7, rosiglitazone inhibited αSMA expression in cultured HSC at concentrations that were in a similar range as required for ACSL4 inhibition (IC_{50} = approx. 100 μM). The relatively high concentration of rosiglitazone required to inhibit HSC activation makes it unlikely that PPAR-γ is involved, since rosiglitazone activates this transcription factor at much lower concentrations (≤10 μM; [23]). However, rosiglitazone is also known to activate an unknown (PPAR-γ independent) mechanism at concentrations around 100 μM [24]. This latter mechanism can be targeted with 15-dPGJ_2 [24]. We therefore compared the inhibitory effects of different concentrations of rosiglitazone and 15-dPGJ_2 on αSMA expression with their effects on ACSL4 activity. Since 15-dPGJ_2 inhibited αSMA expression without affecting ACSL4 activity (Fig. 7), we cannot exclude the possibility that rosiglitazone (partly) inhibits HSC activation by another mechanism, independent of its effect on PUFA-TAG formation.

3.7. Effect of ACSL4 inhibition on eicosanoid secretion by HSCs

TAG-PUFAs may play a role in the AA/eicosanoid metabolism [10,11], and ACSL4 was suggested to increase eicosanoid synthesis in

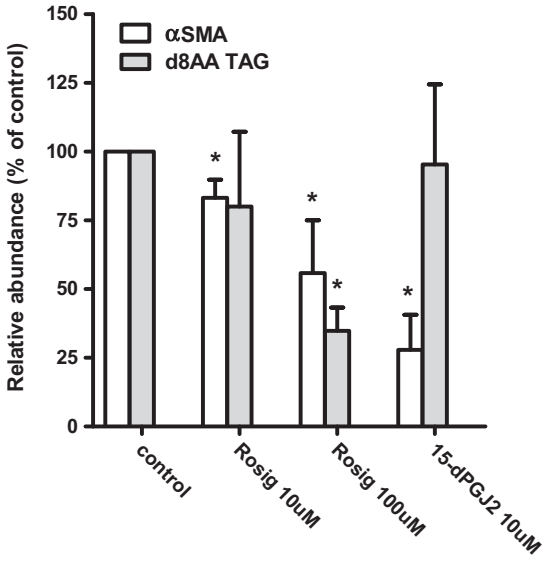

Fig. 7. Effects of rosiglitazone and 15-dPGJ2 on HSC activation and AA incorporation into TAGs. Freshly isolated HSCs were incubated in the absence (control) or presence of rosiglitazone (Rosig) (10 or 100 μM) or 15-deoxy-Δ12,14 prostaglandin J2 (15-dPGJ2; 10 μM) at day 1 and cultured until day 7. Relative gene expression of αSMA (HSC activation marker) was measured by qPCR. In parallel, the incorporation of AA-d8 into TAG was determined by incubation for 24 h with 25 μM AA-d8, similar to Fig. 5. The incorporated d8 label into several representative TAG species with 1, 2 or 3 PUFAs were added. Values are expressed relative to the levels in the control cells and are the means ± SD of 3 experiments. Rosiglitazone or 15-dPGJ2 were added from a 25 mM stock in DMSO to final concentration of 100 μM. In control experiments, the equivalent volume of DMSO was added. *P < 0.05 *t*-test treatment vs control.

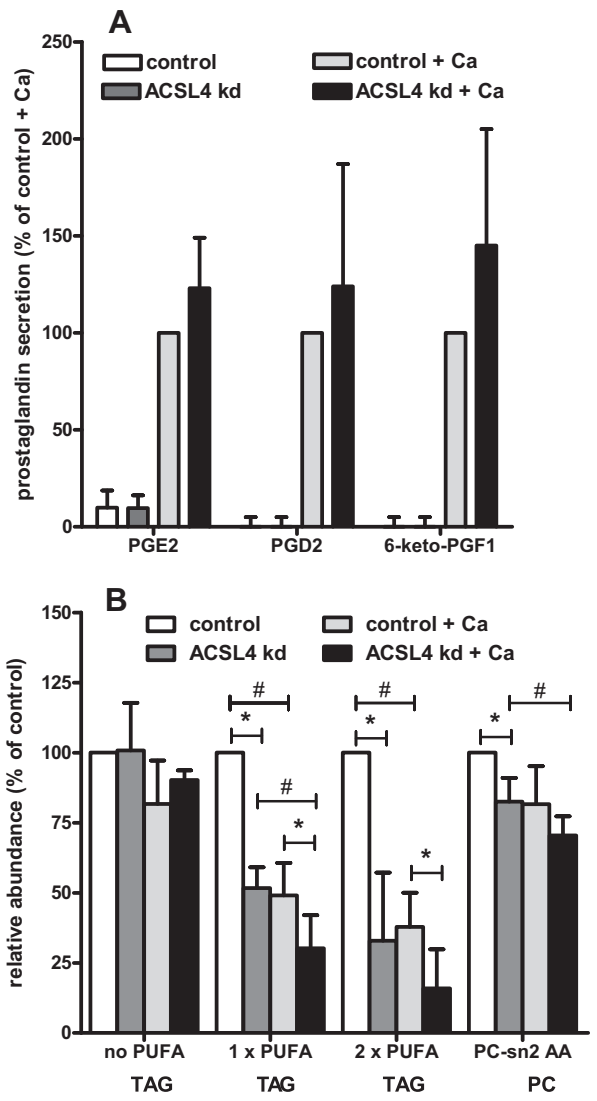

Fig. 8. Effect of *Acsl4* gene silencing on prostaglandin secretion by HSCs Freshly isolated HSCs were transfected with non-targeting (control) or *Acsl4* siRNA at day 2 and cultured until day 7. Subsequently the cells were incubated for 1 h with DMEM containing 0.5% FBS either with or without 10 μM of the Ca^{2+} ionophore A23187. Upper panel: Prostaglandins secreted for 1 h into the low FBS medium were expressed relative to the level secreted by non-targeting (control) cells in the presence of Ca^{2+} ionophore. Lower panel: neutral lipids and phospholipids were extracted and HPLC-MS was performed as described. PC-sn2 AA is the sum of the PC species 36:4, 38:4, and 38:5. Values are expressed relative to the level of lipid present in non-targeting siRNA (control) transfected cells in the absence of Ca^{2+} ionophore. Data are the means of 3 experiments performed in duplicate. Data are the means ± SD of 3 experiments. Lower panel, *P < 0.05 paired *t*-test, ASCL4 kd vs control, #P < 0.05 paired *t*-test, Ca^{2+} ionophore vs no Ca^{2+} ionophore.

tumor cells [20]. We therefore studied the effect of ACSL4 knock down on eicosanoid secretion by activated HSCs. A major eicosanoid detected in the medium of HSCs at day 7 was prostaglandin E_2 (PGE_2). However no difference in the basal PGE_2 secretion between non-targeting and *Acsl4* siRNA transfected HSCs was observed (Fig. 8). Stimulation of Ca^{2+} dependent isoforms of phospholipase A_2 by incubation with a Ca^{2+} ionophore A23187 resulted in a more than 10-fold increase in PGE_2 release by the activated HSCs. As shown in Fig. 8, the secretion of PGE_2 and other prostaglandins was not significantly affected by knock down of ACSL4. We observed also detectable levels of thromboxane B_2 and the hydroxyeicosatetraenoic acids (HETEs), 11-HETE and 15-HETE in the medium of the Ca-ionophore stimulated HSCs, which did also not differ after knock down of ACSL4 (results not shown). To determine whether the eicosanoids after the Ca^{2+} stimulus were derived from the PC and/or the PUFA-TAG pool, we performed lipidomic analyses on the HSCs after incubation with and without the Ca^{2+} ionophore. As shown in Fig. 8, stimulation of phospholipase A_2 activity with Ca^{2+} ionophore caused a relatively strong decrease in TAG-PUFA species, that was larger than the decrease in the PC-AA pool in both non-targeting siRNA transfected cells and in HSCs treated with *Acsl4* siRNA. We could estimate from Fig. 8 and Supplementary Tables 3 and 4, that the observed 50–60% loss in PUFA-TAGs would result in the release of 9–12 nmol of AA/mg protein, whereas a loss of 15–20% of AA-containing phospholipids would release 6–9 nmol of AA/mg protein.

This suggests that PUFAs from the TAG pool are used to replenish the PC-PUFA pool after the stimulation of phospholipase A_2. In that case, prostaglandin secretion will only be affected in HSCs containing no or very low levels of TAG-PUFAs. Therefore, HSCs were pre-incubated for 6 days with 100 μM rosiglitazone, resulting in very low levels of TAG-PUFAs (<20% of control) and 50% of PC-AA (Figs. 6C and D). Under these conditions, Ca^{2+} induced secretion (for 1 h in the absence of rosiglitazone) of PGE_2, PGD_2 and 6-keto-PGF_1-alpha was significantly inhibited by 72 ± 21%, 82 ± 15%, and 69 ± 20%, respectively (n = 3).

4. Discussion

In this paper, we report that ACSL4 is a key enzyme involved in the increase in PUFA-TAGs in activated rat HSCs. This conclusion is based on the observations that ACSL4, which has a preference for PUFAs [8], i) is the only isoform of the ACSL family which is upregulated in activated HSCs, whereas the other isoforms are downregulated, ii) ACSL4 localizes around LDs, and, most importantly, iii) siRNA-mediated gene silencing of *Acsl4* or inhibition of ACSL4 activity by rosiglitazone considerably reduces the amounts of PUFA-TAG species.

Because the different ACSL isoforms have different preferences for fatty acids [8,9], the change in ACSL isoform profile during HSC activation will affect the species profile of the newly formed acyl-CoA pool. In activated HSCs this new acyl-CoA pool will be dominated by PUFA-

CoA species, as PUFAs are the preferred fatty acids of ACSL4. We previously observed that during HSC activation the PUFAs are almost exclusively accumulating in TAGs and not in PLs [7]. We now propose that this increase in PUFA-TAGs is caused by an increase in ACSL4 during HSC activation. Likewise, knock down of ACSL4 in insulin secreting INS 832/13 cells inhibited the incorporation of labeled AA into TAGs but not into PLs [25]. In contrast, overexpression of ACSL4 in arterial smooth muscle cells caused a relatively larger increase in incorporation of labeled AA into PLs as compared to TAGs [20]. There are three main explanations for the differences in response of the TAG and PL species profile to changes in ACSL activity. One explanation states that there is no general acyl-CoA pool for PC and TAG but that specialized pools exist channeling synthesized acyl-CoAs to either TAGs or PLs [26]. This hypothesis requires that different CoA synthesizing enzymes are coupled to either PL or TAG synthesis/remodeling enzymes, for example by differential intracellular localization. Our finding that ACSL4 localizes to large LDs in HSCs, sites of TAG formation [27], supports a channeling hypothesis. Our data are also in agreement with proteomic screens identifying ACSL4 as a LD associated protein [28–31]. Another, not mutually exclusive, explanation is that the enzymes involved in the final step of TAG formation (i.e. DGAT 1 and/or 2) and in PL remodeling (i.e. LPCAT 3 in case of PC [32]) have different affinities for PUFA-CoAs. Indeed, we observed that exogenous AA was incorporated into PC with a higher affinity than into TAGs. The simplest explanation for the observed difference in affinity for exogenous AA is that the final PC and TAG synthesizing enzymes have different affinities for PUFA-CoA. As a consequence, changes in the intra cellular PUFA-CoA concentration, caused by an up- or downregulation of ACSL4 activity, will differentially affect PC and TAG synthesis. The higher affinity for PUFA-PC synthesis will generate smaller effects on the rate of PUFA-PC synthesis as compared to the formation of PUFA-TAG species, as the former is more readily saturated. Especially the formation of TAG species containing 2 and 3 PUFA moieties are expected to be sensitive to variation in PUFA-CoA levels as their formation rate is linear over a large concentration range. A different affinity of the PC and TAG remodeling enzymes for PUFA-CoA also explains our observation that knock-down of ACSL4 and inhibition of ACSL4 with rosiglitazone only caused an appreciable decrease in PUFA-PC species at the low micro molar levels of AA present in the culture medium (Fig. 6), but not in the presence of the higher concentration of exogenous AA-d8 (25 μM) (Figs. 3 and 4). Thirdly, the TAG pool, but not the PL pool, is expandable. This implies that the TAG pool can accommodate the extra PUFA-CoAs formed by ASCL4. In contrast, in the non–expandable PL pool, the higher level of PUFA-CoAs will lead to a somewhat higher rate of replacement, rather than to net higher levels of PUFAs (see Fig. 1B and D).

The role of ACSL4 in the formation of PUFA-TAGs permits an evaluation of the function of the accumulation of PUFA-TAGs during HSC activation by modulating ACSL4 activity. An approximately 80–90% knockdown of ACSL4 obtained by gene silencing caused a strong decrease in PUFA-TAGs, but did not result in a significant change in HSC activation. However this does not exclude a role for ACSL4 or TAG-PUFAs in HSC activation as the remaining PUFA-TAGs may still be sufficient for HSC functioning. A robust inhibition of PUFA-TAG formation was obtained by inhibition of ACSL4 activity using rosiglitazone. Incubation with this ACSL4 inhibitor was indeed associated with a significant inhibition of HSC activation. However rosiglitazone may affect other targets besides ACSL4, which are implicated in the inhibition of a fibrotic response [33,34].

In several types of immune cells esterified AA has been found in isolated LDs [35], and it has been suggested that such LDs serve as an AA reservoir for local activation of essential cellular functions [36]. Furthermore, in several cancer cell lines upregulation of ACSL4 was suggested to control cell proliferation via generation of eicosanoids [37]. HSCs bear some resemblance to dendritic cells involved in the immune system [38]. Therefore, we investigated whether PUFA-TAGs in HSCs play a role in the generation of eicosanoids, allowing signaling with other hepatic cell types like hepatocytes, liver progenitor cells, or macrophages. Gene silencing of *Acsl4* only caused a marginal effect on the secretion of various prostaglandins in activated HSCs. Under the same experimental conditions, we showed that the PUFA-PC levels are not affected, providing an explanation for the observed lack of effect on eicosanoid production by ACSL4 knockdown. In contrast, PUFA-TAG levels are strongly reduced under these conditions, indicating that under conditions of reduced ACSL4 expression, PUFA-TAGs can be used to maintain normal levels PUFA-PC. These experiments point to a possible role of PUFA-TAGs as a reservoir for PL-AA synthesis and thus eicosanoid formation. This was further investigated by generating higher amounts of eicosanoids using Ca^{2+} ionophore A23187. The Ca^{2+} stimulus affected the PUFA-TAG pool much more as compared to the AA-PC pool, suggesting a flux of AA from TAG to PLs or into prostaglandins. A role for TAG-PUFAs as a PUFA buffer was then further corroborated by the experiments where ACSL4 was almost completely inhibited for 6 days with rosiglitazone. Under these conditions, the TAG-PUFA pool was depleted and a strong (70–80%) inhibition of the Ca^{2+} stimulated eicosanoid secretion was observed, despite the presence of 50% PUFA-PC species. Therefore, we suggest that upregulation of ACSL4 during activation serves to protect HSCs against a shortage of PUFAs required for cell growth and eicosanoid production.

Acknowledgements

We would like to acknowledge Jeroen Jansen for technical assistance with the lipid analysis. Real time quantitative PCR was performed at the Department of Clinical Sciences of Companion Animals, Faculty of Veterinary Medicine, Utrecht University, and we thank Ingrid van Gils for technical assistance. Images were acquired at the Center of Cellular Imaging, Faculty of Veterinary Medicine, Utrecht University, on a Leica TCS SPE-II confocal microscope and we thank Esther van't Veld for assistance. 3D rendering of images was performed using Fluorender software. This work was made possible in part by software funded by the NIH: Fluorender: An Imaging Tool for Visualization and Analysis of Confocal Data as Applied to Zebrafish Research, R01-GM098151-01. This work was supported by the seventh framework program of the EU-funded “LipidomicNet” project (proposal number 202272).

Appendix A. Supplementary Data

Supplementary data to this article can be found online at http://dx.doi.org/10.1016/j.bbalip.2014.12.003.

References

[1] W.S. Blaner, S.M. O'Byrne, N. Wongsiriroj, J. Kluwe, D.M. D'Ambrosio, H. Jiang, R.F. Schwabe, E.M.C. Hillman, R. Piantedosi, J. Libien, Hepatic stellate cell lipid droplets: a specialized lipid droplet for retinoid storage, Biochim. Biophys. Acta 1791 (2009) 467–473, http://dx.doi.org/10.1016/j.bbalip.2008.11.001.

[2] S.L. Friedman, Hepatic stellate cells: protean, multifunctional, and enigmatic cells of the liver, Physiol. Rev. 88 (2008) 125–172, http://dx.doi.org/10.1152/physrev.00013.2007.

[3] N. Uyama, Y. Shimahara, N. Kawada, S. Seki, H. Okuyama, Y. Iimuro, Y. Yamaoka, Regulation of cultured rat hepatocyte proliferation by stellate cells, J. Hepatol. 36 (2002) 590–599.

[4] M. Sato, T. Sato, N. Kojima, K. Imai, N. Higashi, D.R. Wang, H. Senoo, 3-D structure of extracellular matrix regulates gene expression in cultured hepatic stellate cells to induce process elongation, Comp. Hepatol. 3 (Suppl. 1) (2004) S4, http://dx.doi.org/10.1186/1476-5926-2-S1-S4.

[5] M. Okuno, H. Moriwaki, S. Imai, Y. Muto, N. Kawada, Y. Suzuki, S. Kojima, Retinoids exacerbate rat liver fibrosis by inducing the activation of latent TGF-beta in liver stellate cells, Hepatology 26 (1997) 913–921, http://dx.doi.org/10.1053/jhep.1997.v26.pm0009328313.

[6] S.L. Friedman, Liver fibrosis — from bench to bedside, J. Hepatol. 38 (Suppl. 1) (2003) S38–S53.

[7] N. Testerink, M. Ajat, M. Houweling, J.F. Brouwers, V.V. Pully, H.J. van Manen, C. Otto, J.B. Helms, A.B. Vaandrager, Replacement of retinyl esters by polyunsaturated triacylglycerol species in lipid droplets of hepatic stellate cells during activation, PLoS ONE 7 (2012) e34945, http://dx.doi.org/10.1371/journal.pone.0034945.

[8] L.O. Li, E.L. Klett, R.A. Coleman, Acyl-CoA synthesis, lipid metabolism and lipotoxicity, Biochim. Biophys. Acta 1801 (2010) 246–251, http://dx.doi.org/10.1016/j.bbalip.2009.09.024.
[9] D.G. Mashek, L.O. Li, R.A. Coleman, Rat long-chain acyl-CoA synthetase mRNA, protein, and activity vary in tissue distribution and in response to diet, J. Lipid Res. 47 (2004-2010), http://dx.doi.org/10.1194/jlr.M600150-JLR200.
[10] P.C. Calder, R.F. Grimble, Polyunsaturated fatty acids, inflammation and immunity, Eur. J. Clin. Nutr. 56 (Suppl. 3) (2002) S14–S19, http://dx.doi.org/10.1038/sj.ejcn.1601478.
[11] H. Harizi, J.B. Corcuff, N. Gualde, Arachidonic-acid-derived eicosanoids: roles in biology and immunopathology, Trends Mol. Med. 14 (2008) 461–469, http://dx.doi.org/10.1016/j.molmed.2008.08.005.
[12] S.A. Farber, E.S. Olson, J.D. Clark, M.E. Halpern, Characterization of Ca^{2+}-dependent phospholipase A2 activity during zebrafish embryogenesis, J. Biol. Chem. 274 (1999) 19338–19346.
[13] L. Riccalton-Banks, R. Bhandari, J. Fry, K.M. Shakesheff, A simple method for the simultaneous isolation of stellate cells and hepatocytes from rat liver tissue, Mol. Cell. Biochem. 248 (2003) 97–102.
[14] F.G. van Steenbeek, L. Van den Bossche, G.C. Grinwis, A. Kummeling, I.H. van Gils, M.J. Koerkamp, D. van Leenen, F.C. Holstege, L.C. Penning, J. Rothuizen, P.A. Leegwater, B. Spee, Aberrant gene expression in dogs with portosystemic shunts, PLoS ONE 8 (2013) e57662, http://dx.doi.org/10.1371/journal.pone.0057662.
[15] E.G. Bligh, W.J. Dyer, A rapid method of total lipid extraction and purification, Can. J. Biochem. Physiol. 37 (1959) 911–917.
[16] K. Retra, O.B. Bleijerveld, R.A. van Gesteil, A.G.M. Tielens, J.J. van Hellemond, J.F. Brouwers, A simple and universal method for the separation and identification of phospholipid molecular species, Rapid Commun. Mass Spectrom. 22 (2008) 1853–1862, http://dx.doi.org/10.1002/rcm.3562.
[17] M. Kates, Techniques of lipidology: isolation, analysis and identification of lipids, in: R.H. Burdon, P.H. Van Knippenberg (Eds.), *In* Laboratory Techniques in Biochemistry and Molecular Biology, 2nd ed., 125, Elsevier, Amsterdam, 1986.
[18] H. Aardema, F. Lolicato, C.H. van de Lest, J.F. Brouwers, A.B. Vaandrager, H.T. van Tol, B.A. Roelen, P.L. Vos, J.B. Helms, B.M. Gadella, Bovine cumulus cells protect maturing oocytes from increased fatty acid levels by massive intracellular lipid storage, Biol. Reprod. 88 (2013) 164 1–164 15, http://dx.doi.org/10.1095/biolreprod.112.106062.
[19] J.C. de Grauw, C.H. van de Lest, P.R. van Weeren, A targeted lipidomics approach to the study of eicosanoid release in synovial joints, Arthritis Res. Ther. 13 (2011) R123, http://dx.doi.org/10.1186/ar3427.
[20] D.L. Golej, B. Askari, F. Kramer, S. Barnhart, A. Vivekanandan-Giri, S. Pennathur, K.E. Bornfeldt, Long-chain acyl-CoA synthetase 4 modulates prostaglandin E(2) release from human arterial smooth muscle cells, J. Lipid Res. 52 (2011) 782–793, http://dx.doi.org/10.1194/jlr.M013292.
[21] B. Askari, J.E. Kanter, A.M. Sherrid, D.L. Golej, A.T. Bender, J. Liu, W.A. Hsueh, J.A. Beavo, R.A. Coleman, K.E. Bornfeldt, Rosiglitazone inhibits acyl-CoA synthetase activity and fatty acid partitioning to diacylglycerol and triacylglycerol via a peroxisome proliferator-activated receptor-gamma-independent mechanism in human arterial smooth muscle cells and macrophages, Diabetes 56 (2007) 1143–1152, http://dx.doi.org/10.2337/db06-0267.
[22] F.J. Eng, S.L. Friedman, I. Fibrogenesis, New insights into hepatic stellate cell activation: the simple becomes complex, Am. J. Physiol. Gastrointest. Liver Physiol. 279 (2000) G7–G11.
[23] L. Al-Alem, R.C. Southard, M.W. Kilgore, T.E. Curry, Specific thiazolidinediones inhibit ovarian cancer cell line proliferation and cause cell cycle arrest in a PPARgamma independent manner, PLoS ONE 6 (2011) e16179, http://dx.doi.org/10.1371/journal.pone.0016179.
[24] H.E. Ferguson, A. Kulkarni, G.M. Lehmann, T.M. Garcia-Bates, T.H. Thatcher, K.R. Huxlin, R.P. Phipps, P.J. Sime, Electrophilic peroxisome proliferator-activated receptor-gamma ligands have potent antifibrotic effects in human lung fibroblasts, Am. J. Respir. Cell Mol. Biol. 41 (2009) 722–730, http://dx.doi.org/10.1165/rcmb.2009-0006OC.
[25] E.L. Klett, S. Chen, M.L. Edin, L.O. Li, O. Ilkayeva, D.C. Zeldin, C.B. Newgard, R.A. Coleman, Diminished Acyl-CoA synthetase isoform 4 activity in INS 832/13 cells reduces cellular epoxyeicosatrienoic acid levels and results in impaired glucose-stimulated insulin secretion, J. Biol. Chem. 288 (2013) 21618–21629, http://dx.doi.org/10.1074/jbc.M113.481077.
[26] D.G. Mashek, L.O. Li, R.A. Coleman, Long-chain acyl-CoA synthetases and fatty acid channeling, Futur. Lipidol. 2 (2007) 465–476.
[27] F. Wilfling, H. Wang, J.T. Haas, N. Krahmer, T.J. Gould, A. Uchida, J.X. Cheng, M. Graham, R. Christiano, F. Frohlich, X. Liu, K.K. Buhman, R.A. Coleman, J. Bewersdorf, R.V. Farese Jr., T.C. Walther, Triacylglycerol synthesis enzymes mediate lipid droplet growth by relocalizing from the ER to lipid droplets, Dev. Cell 24 (2013) 384–399, http://dx.doi.org/10.1016/j.devcel.2013.01.013.
[28] P. Liu, Y. Ying, Y. Zhao, D.I. Mundy, M. Zhu, R.G. Anderson, Chinese hamster ovary K2 cell lipid droplets appear to be metabolic organelles involved in membrane traffic, J. Biol. Chem. 279 (2004) 3787–3792, http://dx.doi.org/10.1074/jbc.M311945200.
[29] D.L. Brasaemle, G. Dolios, L. Shapiro, R. Wang, Proteomic analysis of proteins associated with lipid droplets of basal and lipolytically stimulated 3T3-L1 adipocytes, J. Biol. Chem. 279 (2004) 46835–46842, http://dx.doi.org/10.1074/jbc.M409340200.
[30] E. Umlauf, E. Csaszar, M. Moertelmaier, G.J. Schuetz, R.G. Parton, R. Prohaska, Association of stomatin with lipid bodies, J. Biol. Chem. 279 (2004) 23699–23709, http://dx.doi.org/10.1074/jbc.M310546200.
[31] S.Y. Cho, E.S. Shin, P.J. Park, D.W. Shin, H.K. Chang, D. Kim, H.H. Lee, J.H. Lee, S.H. Kim, M.J. Song, I.S. Chang, O.S. Lee, T.R. Lee, Identification of mouse Prp19p as a lipid droplet-associated protein and its possible involvement in the biogenesis of lipid droplets, J. Biol. Chem. 282 (2007) 2456–2465, http://dx.doi.org/10.1074/jbc.M608042200.
[32] H. Shindou, D. Hishikawa, T. Harayama, M. Eto, T. Shimizu, Generation of membrane diversity by lysophospholipid acyltransferases, J. Biochem. 154 (2013) 21–28, http://dx.doi.org/10.1093/jb/mvt048.
[33] A. Galli, D.W. Crabb, E. Ceni, R. Salzano, T. Mello, G. Svegliati-Baroni, F. Ridolfi, L. Trozzi, C. Surrenti, A. Casini, Antidiabetic thiazolidinediones inhibit collagen synthesis and hepatic stellate cell activation in vivo and in vitro, Gastroenterology 122 (2002) 1924–1940.
[34] T. Miyahara, L. Schrum, R. Rippe, S. Xiong, H.F. Yee Jr., K. Motomura, F.A. Anania, T.M. Willson, H. Tsukamoto, Peroxisome proliferator-activated receptors and hepatic stellate cell activation, J. Biol. Chem. 275 (2000) 35715–35722, http://dx.doi.org/10.1074/jbc.M006577200.
[35] P.T. Bozza, K.G. Magalhaes, P.F. Weller, Leukocyte lipid bodies — biogenesis and functions in inflammation, Biochim. Biophys. Acta 1791 (2009) 540–551, http://dx.doi.org/10.1016/j.bbalip.2009.01.005.
[36] H.J. van Manen, Y.M. Kraan, D. Roos, C. Otto, Single-cell Raman and fluorescence microscopy reveal the association of lipid bodies with phagosomes in leukocytes, Proc. Natl. Acad. Sci. U. S. A. 102 (2005) 10159–10164, http://dx.doi.org/10.1073/pnas.0502746102.
[37] P.M. Maloberti, A.B. Duarte, U.D. Orlando, M.E. Pasqualini, A.R. Solano, C. Lopez-Otin, E.J. Podesta, Functional interaction between acyl-CoA synthetase 4, lipooxygenases and cyclooxygenase-2 in the aggressive phenotype of breast cancer cells, PLoS ONE 5 (2010) e15540, http://dx.doi.org/10.1371/journal.pone.0015540.
[38] H.S. Chou, C.C. Hsieh, H.R. Yang, L. Wang, Y. Arakawa, K. Brown, Q. Wu, F. Lin, M. Peters, J.J. Fung, L. Lu, S. Qian, Hepatic stellate cells regulate immune response by way of induction of myeloid suppressor cells in mice, Hepatology 53 (2011) 1007–1019, http://dx.doi.org/10.1002/hep.24162.